



# Cluster Partition-Based Zonal Voltage Control for Distribution Networks With High Penetrated PVs

Xingyu Zhao, Chuanliang Xiao\*, Ke Peng, Jiajia Chen and Xinhui Zhang

School of Electronic Engineering, Shandong University of Technology, Zibo, China

With the high penetrated photovoltaics (PVs) accessing distribution networks (DNs) in the future, the overvoltage of distribution network will be more serious, and the voltage control will be more complex. To solve this problem, a cluster partition-based zonal voltage control method for DN is proposed in this study. First, a cluster partition method using a comprehensive performance index is proposed: in terms of DN structure, a global density quality function index is introduced to measure the coupling degree of nodes in clusters. In terms of cluster function, the inconsistency coefficient index is presented to reflect the PV output characteristics, and a node membership function index is presented to limit the scale of the cluster. Then, the DN cluster partition is carried out under the fast Newman (FN) algorithm. Second, a second-order cone programming (SOCP) model of voltage control is established to maximize the PV consumption in each cluster. To achieve the coordinated optimization of clusters, an iterative optimization strategy among clusters is proposed. Finally, the effectiveness and rationality of the proposed method are verified in a 10 kV actual feeder system in Zhejiang Province, China.

**Keywords:** distributed network, photovoltaic generation, cluster partition, distributed optimization, voltage control

## OPEN ACCESS

### Edited by:

Yunfei Mu,  
Tianjin University, China

### Reviewed by:

Qianlong Zhu,  
Anhui University, China  
Zhijian Feng,  
Qingdao University, China

### \*Correspondence:

Chuanliang Xiao  
xiaocl@sdut.edu.cn

### Specialty section:

This article was submitted to  
Smart Grids,  
a section of the journal  
Frontiers in Energy Research

**Received:** 21 March 2022

**Accepted:** 04 April 2022

**Published:** 02 May 2022

### Citation:

Zhao X, Xiao C, Peng K, Chen J and  
Zhang X (2022) Cluster Partition-  
Based Zonal Voltage Control for  
Distribution Networks With High  
Penetrated PVs.  
Front. Energy Res. 10:900824.  
doi: 10.3389/fenrg.2022.900824

## 1 INTRODUCTION

In order to promote the realization of peaking and carbon neutrality goals, China will carry out the development of roof-distributed PVs for the whole county. However, the integration of large-scale PVs aggravates the overvoltage in the DN (Wang et al., 2021), and the voltage control model turns into a high-dimensional complex model (Liao et al., 2017; Li et al., 2018), which is difficult to solve. Therefore, the investigation of voltage control strategies for active distribution networks (ADNs) with a high penetration of PVs is necessary to improve the consumption of PVs. Zonal voltage control (Han et al., 2019) provides an effective solution for solving the complex voltage control. Under the network partition, the high-dimensional voltage control model can be transformed into several subproblems which are easy to be solved (Xiao, 2020). Zonal voltage control mainly exists in two aspects: network partition and subnetwork voltage regulation.

To implement the zonal voltage control, the network partition is first carried out. In terms of the network partition index, the DN structure and power balance are the main basis for a network partition. Hu et al. (2021) used the reactive voltage sensitivity matrix to express the electrical coupling degree between nodes, and the sensitive nodes are found out to complete the network partition. Dou et al. (2018) proposed a division index system of virtual cluster, including the spatial location, output characteristics, and response mode of PVs. Kou et al. (2019) proposed the network partition indexes which include the net load of nodes and active and reactive power regulation capacity of PVs. Chai et al. (2007) proposed the cluster performance index. The index considers the electrical distance

between nodes and regional voltage regulating ability, which can ensure each cluster solves the voltage violations within the clusters. In the context of PV accessing in the whole counties, the scale of PVs in DNs is continuously expanded, the influence of PVs on network partition cannot be ignored. Therefore, it is not enough to employ the electrical distance and power balance as the network partition index. If the consistency of PV output and nodal voltage in the cluster can be considered during the network partition, the output of the subnetwork will be more smooth and controllable. In terms of network partition algorithms, there are three main types: intelligent algorithms, clustering algorithms, and community discovery algorithms of complex networks. Bi et al. (2019) proposed an improved genetic algorithm, which can find the optimal network partition according to the state of tie switch. Although the amount of calculation is reduced, this algorithm has a long time scale, which is not suitable for real-time optimization. Yan et al. (2021) used the Tabu search algorithm to complete the network partition. But this algorithm cannot automatically generate the optimal number of clusters, which can lead to an inaccurate result. Wang et al. (2021) proposes a fast-unfolding clustering algorithm for cluster partitioning, which employs the complex network modularity function to avoid setting the threshold value. When the network structure changes, the algorithm is no longer applicable. In different scenarios, and the time scale and accuracy of the network partition are different. For the zonal voltage control of DNs, the voltage control belongs to a real-time optimization, which requires a short-time scale of network partition. Therefore, determining how to establish a network partition algorithm with fast computing speed and accurate performance is the key to achieving zonal voltage control.

After DNs are partitioned into several subnetworks, the zonal voltage control method can be applied. The zonal voltage control mainly focuses on the optimization within subnetworks and the coordination among subnetworks. Xiao et al. (2017) adopted the zonal voltage control strategy of “maximize reactive power regulating first, and then minimize active power curtailing.” Although the control process is simplified, the active power–reactive power interaction between subnetworks is not considered. According to the overvoltage degree, Li et al. (2021) proposed a voltage regulation control strategy based on the energy storage cluster. Autonomous optimization is realized by utilizing the energy storage system in clusters, but the coordination between clusters is not considered. Chai et al. (2019) used the alternating direction method of multipliers (ADMM) to optimize the zonal voltage between upstream and downstream clusters, which only achieves the coordination between adjacent clusters. With the high penetrated PVs accessing distribution networks, it is necessary to further establish a reasonable and effective coordination strategy among clusters. Therefore, realizing the independent voltage control in each subnetwork and the coordinating control among the subnetworks deserves deep research.

In light of the aforementioned issues, this study proposes a cluster partition-based zonal voltage control method for DNs. The main contributions of this study are summarized as follows:

- 1) Based on the community partition theory, a cluster partition method combined with the cluster comprehensive performance index and FN algorithm is proposed. The electrical information of the network structure and the impact of PVs on the partitioning solutions are considered, and the size of each subnetwork can be restricted.
- 2) A SOCP-based voltage control model aiming at the maximum PV consumption in the cluster is established. The high-dimensional voltage control model of the whole DN is transformed into several subproblems within the clusters, which are easily solved.
- 3) An iterative optimization-based active power coordination strategy among clusters is proposed to realize the coordination among different clusters. The maximum PV consumption for all clusters can be guaranteed.

The remainder of this study is organized as follows. In **Section 2**, a comprehensive performance index-based cluster partition method is proposed. In **Section 3**, an independent optimization model in the cluster is proposed. In **Section 4**, the active power coordination and interaction strategy among clusters is proposed. The case study is described in **Section 5**, and a 10 kV actual feeder network is used for simulation verification, followed by discussion and conclusions in **Section 6**.

## 2 COMPREHENSIVE PERFORMANCE INDEX-BASED CLUSTER PARTITION METHOD

### 2.1 Comprehensive Performance Index of Cluster Partition

In order to solve the problem that the factors of the existing cluster partition index are not comprehensive, in this study, based on the DN structure and cluster function, the comprehensive performance index is proposed to complete the cluster partition. The comprehensive performance index is composed of the global density quality function index, the inconsistency coefficient index, and the node membership function index.

The global density quality function is selected to measure the coupling degree of nodes in clusters according to the DN, so as to satisfy the structural principle which means that the nodes with a strong coupling degree should be divided into the same clusters, and nodes with a weak coupling degree should be divided into different clusters. First, the global internal density quality function  $Q_{GD}^i$  and the global external density quality function  $Q_{GD}^e$  are defined, where  $Q_{GD}^i$  represents the coupling degree of nodes within the cluster and  $Q_{GD}^e$  represents the coupling degree of nodes between clusters.

$$Q_{GD}^i = \frac{\sum_{k=1}^K \sum_{x \in V_k} \sum_{y \in V_k} A_{xy}}{\sum_i \sum_j A_{ij}}, \quad (1)$$

$$Q_{GD}^e = \frac{\sum_{k=1}^K \sum_{x \in V_k} \sum_{y \in V - V_k} A_{xy}}{\sum_i \sum_j A_{ij}}, \quad (2)$$

where  $k$  is the number of clusters,  $V_k$  represents the  $k$ -th cluster,  $A_{xy}$  represents the weight of the edges of nodes  $x$  and  $y$ ,  $\sum_{k=1}^K \sum_{x \in V_k} \sum_{y \in V-V_k} A_{xy}$  represents the sum of edge weights of all nodes in the cluster  $K$ ,  $\sum_{k=1}^K \sum_{x \in V_k} \sum_{y \in V-V_k} A_{xy}$  represents the sum of edge weights of all nodes in different clusters,  $A_{ij}$  represents the weight of the edges of nodes  $i$  and  $j$ , and  $\sum_i \sum_j A_{ij}$  represents the sum of edge weights of all nodes in the whole network.

In this study, the edge weight of the DN is determined by the active voltage sensitivity matrix  $S_{PV}$ , which can be got from Xiao et al. (2017). In order to reflect the coupling degree between nodes, the average value of edge weight is used to represent the weight  $A_{ij}$ :

$$A_{ij} = \frac{S_{PV}^{ij} + S_{PV}^{ji}}{2}, \tag{3}$$

where the value of  $Q_{GD}^i$  and  $Q_{GD}^e$  belongs to (0,1). As  $Q_{GD}^i$  is close to 1, it indicates that the nodes in a cluster have a strong coupling degree. As  $Q_{GD}^e$  is close to 0, indicates that the nodes in different clusters have a weak coupling degree. The global density quality function index  $Q_{GD}$  is defined as follows:

$$Q_{GD} = \frac{1}{2} (Q_{GD}^i + 1 - Q_{GD}^e). \tag{4}$$

The value of  $Q_{GD}$  belongs to (0,1). As  $Q_{GD}$  is close to 1, it indicates that in the same clusters, the nodes have a strong coupling degree and in the different clusters, the nodes have a weak coupling degree, that is, the larger the value of  $Q_{GD}$ , the better the partition result.

Due to the strong fluctuation of PV output, it is difficult to ensure that the clustering results can satisfy the DN topology constraints. If the PV nodes with inconsistent output are partitioned into the same cluster, the PV output in each cluster will be smoother, and the regulation ability of clusters can be increased. Therefore, the inconsistency coefficient index  $X$  is proposed to describe the variation trend of PV output in the cluster at different times.

$$X = \frac{1}{\Delta T} \sum_{t=2}^T \sum_{i \in V_k} \sum_{j \in V_k} f_t(P^i, P^j) / (T - 1), \tag{5}$$

where  $P^i$  and  $P^j$  are the output sequences of PV  $i$  and PV  $j$  in the network,  $T$  is the sampling number of PV output in the whole day, and  $\Delta T$  is the sampling time interval, which is set to 15 min. The expression of  $f_t(P^i, P^j)$  is given as follows:

$$f_t(P^i, P^j) = \begin{cases} 1, & (P_t^i - P_{t-1}^i)(P_t^j - P_{t-1}^j) < 0 \\ 0, & (P_t^i - P_{t-1}^i)(P_t^j - P_{t-1}^j) \geq 0 \end{cases}, \tag{6}$$

where  $f_t(P^i, P^j)$  is the inconsistency of the output curve trend between PV  $i$  and PV  $j$  during the  $t$ -th to the  $t-1$  sampling point within a cluster. When the output curve trend of two PVs is inconsistent (one rising and one falling),  $f_t(P^i, P^j)$  is taken as 1, and  $f_t(P^i, P^j)$  is taken as 0 when they are consistent.

A suitable scale of cluster will affect the difficulty of subsequent zonal voltage control. The balance of nodal size in clusters will reduce the complexity of zonal voltage control. Therefore, in

order to judge the nodal size of each cluster, a node membership index is established:

$$M = \frac{\mu(x, V[x])}{\mu(x, V - V[x])}, \tag{7}$$

$$\mu(x, V[x]) = \frac{1}{|V[x]|} \sum_{y \in V[x]} A_{xy}, \tag{8}$$

$$\mu(x, V - V[x]) = \frac{1}{|V - V[x]|} \sum_{y \in V - V[x]} A_{xy}, \tag{9}$$

where  $V[x]$  represents the cluster which node  $x$  belongs to, that is,  $x \in V[x]$ ;  $|V[x]|$  represents the sum of total edges between nodes in the cluster, where node  $x$  belongs to;  $\mu(x, V[x])$  indicates the membership degree of the nodes connected to  $x$  in the same cluster  $V[x]$ ;  $V - V[x]$  represents the cluster which does not contain node  $x$ ;  $|V - V[x]|$  indicates the sum of edges between nodes within clusters, except  $V[x]$ ; and  $\mu(x, V - V[x])$  indicates the membership degree of node  $y$  in cluster  $V - V[x]$ .

Based on the aforementioned indexes, the comprehensive performance index is defined as follows:

$$\omega = \omega_1 Q_{GD} + \omega_2 X + \omega_3 M, \tag{10}$$

where  $\omega_1$ ,  $\omega_2$ , and  $\omega_3$  are the weights of global density quality function index, inconsistency coefficient index, and node membership index, respectively, which meet  $0 \leq \omega_1$ ;  $\omega_2$ ;  $\omega_3 \leq 1$  and  $\omega_1 + \omega_2 + \omega_3 = 1$ .

## 2.2 Cluster Partition Algorithm

Community structures are formed by the aggregation of network nodes, which generally utilize regional coupling of physical, chemical, or social interaction relations (Cohen, 2009). The community should satisfy that the nodes with a strong coupling degree belong to the same clusters, and nodes with a weak coupling degree belong to different clusters. A power network is also a complex network composed of points and edges, in which the point corresponds to the node in the network, and the edge corresponds to the connecting line between nodes (Liu, 2019). The community not only reflects the structural characteristics of the network but also reveals the internal relations of the network. Based on the community discovery algorithm, the community structure, which has a close connection within the community and a sparse connection between communities, can be analyzed. The FN algorithm is a complex network community partition algorithm based on a local search proposed by Newman et al. (2004). The steps of using the FN algorithm to divide clusters are as follows:

- Step 1: Each node in the network is regarded as a separate cluster, and the initial comprehensive performance index value  $\omega^0$  is calculated according to **Eq. 10**.
- Step 2: For node  $i$ , node  $j$  is selected randomly from the remaining nodes to merge into a node pair. The comprehensive performance index  $\omega^1$  is calculated. Then calculate the value  $\Delta\omega = \omega^1 - \omega^0$ .

- Step 3: Step 2 is repeated for all node pairs. The node pair with the largest  $\Delta\omega$  will be merged into a cluster and referred to as an individual node.
- Step 4: Steps 1-3 are repeated until the comprehensive performance index value for all node pairs does not increase. The optimal cluster partition and the associated comprehensive performance index value can be obtained.

### 3 ZONAL VOLTAGE CONTROL MODEL IN CLUSTERS

#### 3.1 Objective Function

For the overvoltage in the DN, a SOCP-based voltage control model is established with the objective function to maximize the PV consumption. Based on the cluster partition, combined with the regulation capacity of energy storage, the objective functions of clusters can be established as follows:

$$F = \max \left\{ \sum_{i=1}^{n_K^{PV}} P_{i,t}^{PV} - P_{ESS,t} - P_{loss,t} \right\}, \quad (11)$$

where  $n_K^{PV}$  is the number of installed PVs in cluster  $K$ ,  $P_{i,t}^{PV}$  is the output power of PV  $i$  at time  $t$ ,  $P_{ESS,t}$  is the energy storage power at time  $t$ , and  $P_{loss,t}$  is the network loss at time  $t$ .

#### 3.2 Constraints of the Proposed Model

##### 1) Power flow constraints of DN

The traditional nonlinear power flow model can be transformed into a SOCP power flow model by second-order cone relaxation (Peng et al., 2021).

$$\begin{cases} P_{ij,t}^2 + Q_{ij,t}^2 = L_{ij,t} U_{i,t}^2 \\ U_{i,t}^2 = u_{i,t} \end{cases} = \left\| \begin{matrix} 2P_{ij,t} \\ 2Q_{ij,t} \\ L_{ij,t} - u_{i,t} \end{matrix} \right\|_2 \leq L_{ij,t} + u_{i,t}, \forall (i,j) \in \chi, \quad (12)$$

$$P_{PV,j,t} - P_{L,j,t} - P_{ESS,j,t} = \sum_{i \in \Phi(j)} P_{j,t} - \sum_{i \in \Lambda(j)} (P_{ij,t} - r_{ij} L_{ij,t}), \forall j \in \Pi_K^P, \quad (13)$$

$$P_{PV,j,t}^* - P_{L,j,t} - P_{ESS,j,t} = \sum_{i \in \Phi(j)} P_{j,t} - \sum_{i \in \Lambda(j)} (P_{ij,t} - r_{ij} L_{ij,t}), \forall j \in \Pi_K^P, \quad (14)$$

$$Q_{PV,j,t} - Q_{L,j,t} = \sum_{i \in \Phi(j)} Q_{j,t} - \sum_{i \in \Lambda(j)} (Q_{ij,t} - x_{ij} L_{ij,t}), \forall j \in \Pi, \quad (15)$$

$$(U^{min})^2 \leq u_{i,t} \leq (U^{max})^2, \forall j \in \Pi, \quad (16)$$

$$L_{ij,t} \leq (I_{ij}^{max})^2, \forall (i,j) \in \chi. \quad (17)$$

In the aforementioned constraints, Eq. 12 represents the second-order cone relaxation transformation of branch power flow, where  $L_{ij,t}$  represents squared current magnitude of line  $i$ - $j$  at time  $t$ ;  $P_{ij,t}$  and  $Q_{ij,t}$  represent the active power and reactive power of the line from node  $i$  to node  $j$  at time  $t$ , respectively;  $U_{i,t}$  represents the voltage amplitude on node  $i$  at time  $t$ ;  $u_{i,t}$  represents

the square of the voltage amplitude on node  $i$  at time  $t$ ; and  $\chi$  represents all line sets. Eqs 13–15 represent the injection power balance equation of active and reactive nodes, where  $\Phi(j)$  and  $\Lambda(j)$  represent the parent branch set and child branch set of node  $j$ , respectively;  $P_{PV,j,t}$  represents the adjusted active power generation of the  $j$ -th PV node at time  $t$ ;  $P_{PV,j,t}^*$  represents the output active power of the  $j$ -th PV at time  $t$ , which is the constant value;  $Q_{PV,j,t}$  represents the reactive power regulation amount of the PV inverter of the  $j$ -th PV at time  $t$ , which is the constant value;  $\Pi$  represents a collection of all nodes;  $\Pi_K^P$  represents the collection of all nodes in cluster  $K$ ;  $P_{L,j,t}$  and  $Q_{L,j,t}$  represent the active and reactive load demand of the  $j$ -th node at time  $t$ ;  $P_{ESS,j,t}$  represents the energy storage absorbed power at the  $j$ -th node at time  $t$ ; and  $r_{ij}$  and  $x_{ij}$  represent the resistance and reactance of line  $i$ - $j$ . Eqs 16, 17 represent the node voltage amplitude and branch current constraints, where  $I_{ij}^{max}$  represents the maximum current of line  $i$ - $j$ .

##### 2) Upper and lower limits of PV output:

$$0 \leq P_{PV,i,t} \leq P_{PV,i,t}^{max}, \quad (18)$$

where  $P_{PV,i,t}^{max}$  is the upper limit value of active power output of PV  $i$  at time  $t$ .

##### 3) Energy storage state constraints:

$$S_{OC,min} \leq S_{OC,t} \leq S_{OC,max}, \quad (19)$$

$$-P_{ESS,N} \leq P_{ESS,t} \leq P_{ESS,N}, \quad (20)$$

where  $S_{OC,t}$  is the energy storage state of charge at time  $t$ ;  $S_{OC,max}$  and  $S_{OC,min}$  are the upper and lower limits of the energy storage state of charge, respectively;  $P_{ESS,t}$  is the energy storage power at time  $t$ ; and  $P_{ESS,N}$  is the rated power of energy storage.

### 4 ITERATIVE OPTIMIZATION-BASED ACTIVE POWER COORDINATION STRATEGY OF CLUSTERS

To realize the coordination among clusters, an iterative optimization-based active power coordination strategy among clusters is proposed, which takes advantage of the weak coupling between clusters. The specific process of the proposed strategy is shown in Figure 1.

Step 1: Based on the cluster partition, check whether the node voltage in each cluster exceeds the voltage limit. If the node voltage is within the normal range, it ends; if there exists overvoltage, proceed to the next step.

Step 2: The clusters with overvoltage are recorded as  $C^V = \{C_1^V, C_2^V, \dots, C_K^V, \dots, C_N^V\}$ . Then, each cluster in  $C^V$  optimizes the objective of Eq. 11 to obtains the optimal output power of PV  $P_{PV}^0 = \{P_{C_1^V, PV}^0, P_{C_2^V, PV}^0, \dots, P_{C_K^V, PV}^0, \dots, P_{C_N^V, PV}^0\}$ , and the charging power of stored energy  $P_{ESS}^0 = \{P_{C_1^V, ESS}^0, P_{C_2^V, ESS}^0, \dots, P_{C_K^V, ESS}^0, \dots, P_{C_N^V, ESS}^0\}$ .

Step 3: Based on the intra-cluster optimal solution  $P_{PV}^0$  and  $P_{ESS}^0$ , a power flow calculation is carried out for the DN after the

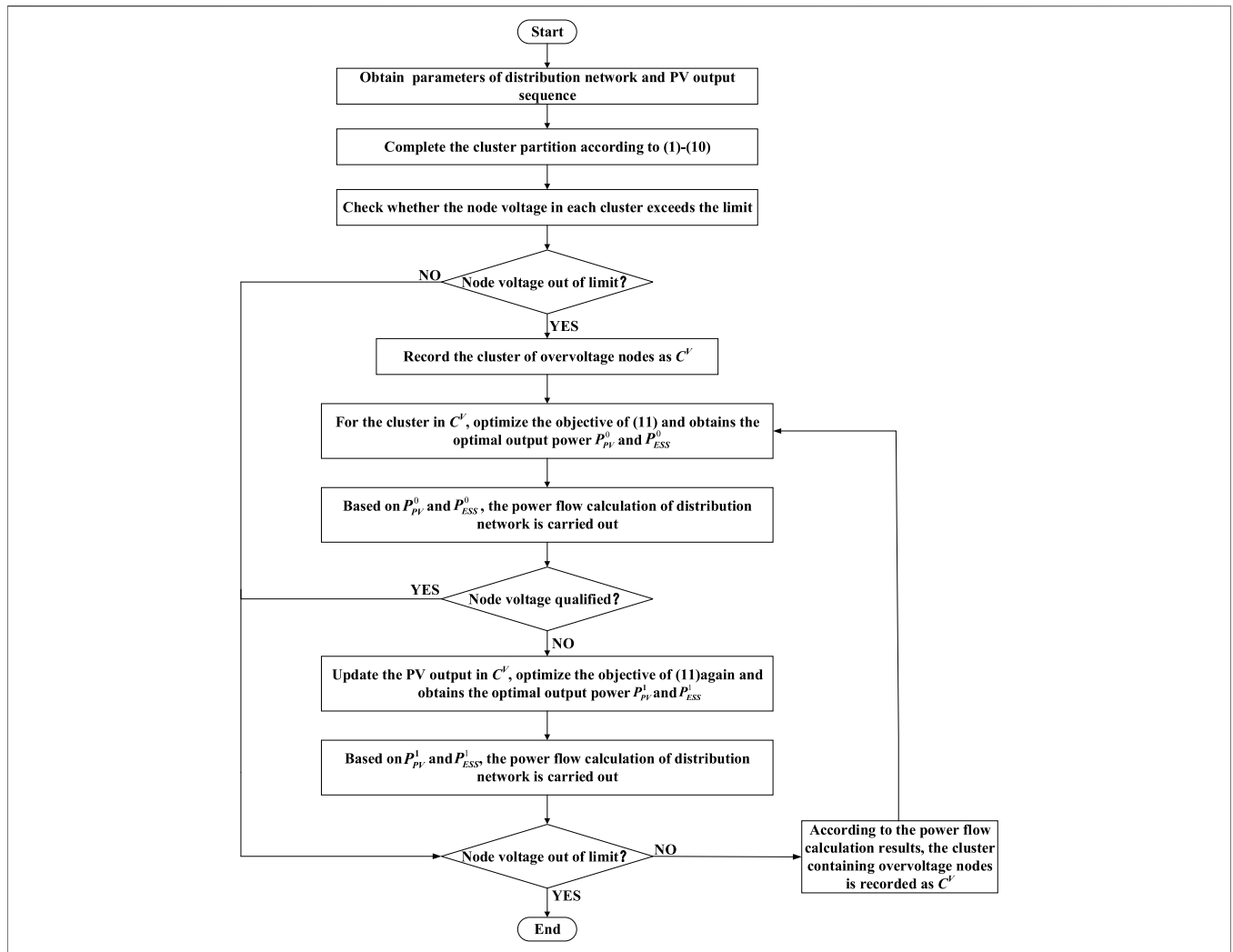


FIGURE 1 | Flowchart of the proposed voltage control.

active power cutting of the PV in cluster  $C^V$ . When the voltage of the whole network is qualified, it ends.

Otherwise, go to the next step.

Step 4: Taking  $P_{PV}^0$  as the initial value, each cluster in  $C^V$  optimizes the objective of Eq. 11 again to obtains the best output power of PV  $P_{PV}^1 = \{P_{C_1^V, PV}^1, P_{C_2^V, PV}^1, \dots, P_{C_K^V, PV}^1, \dots, P_{C_N^V, PV}^1\}$ , and the charging power of stored energy  $P_{ESS}^1 = \{P_{C_1^V, ESS}^1, P_{C_2^V, ESS}^1, \dots, P_{C_K^V, ESS}^1, \dots, P_{C_N^V, ESS}^1\}$ .

Step 5: Perform a power flow calculation based on the optimized results in step 4. If the voltage of the whole network is qualified, it ends; otherwise, proceed to the next step.

Step 6: Repeat steps 2-5 until all node voltages are within the normal range.

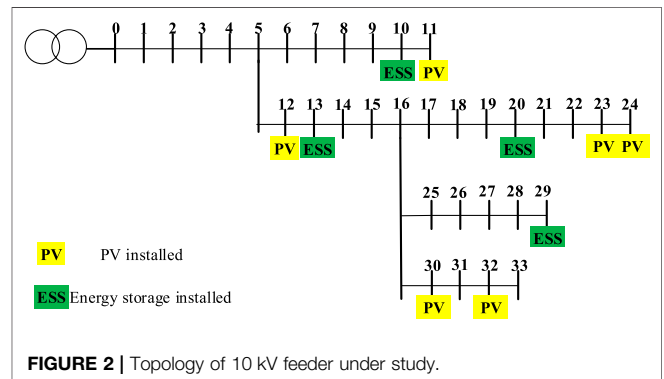


FIGURE 2 | Topology of 10 kV feeder under study.

**TABLE 1** | Capacity of installed PVs.

| Node location | 11  | 12  | 23  | 24  | 30  | 32    |
|---------------|-----|-----|-----|-----|-----|-------|
| Capacity (kW) | 500 | 500 | 500 | 500 | 500 | 1,500 |

**TABLE 2** | Capacity of installed energy storage.

| Node location | 10  | 13  | 20  | 29    |
|---------------|-----|-----|-----|-------|
| Capacity (kW) | 300 | 300 | 300 | 1,000 |

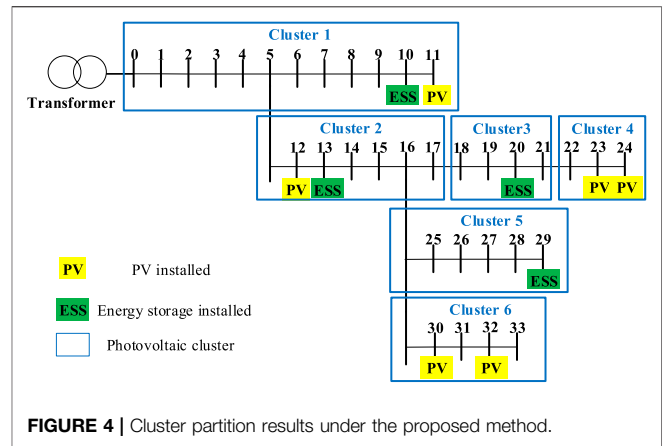
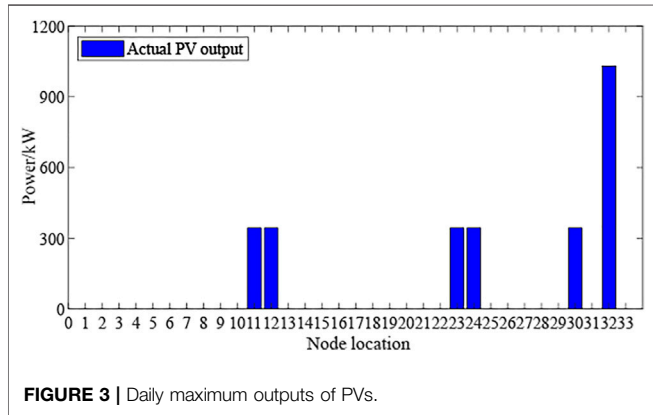


**TABLE 4** | Results of cluster partition under different indexes.

| Cluster | Node                              |                                   |
|---------|-----------------------------------|-----------------------------------|
|         | $\omega$                          | $\rho$                            |
| 1       | 1, 2, 3, 4, 5, 6, 7, 8, 9, 10, 11 | 1, 2, 3, 4, 5, 6, 7, 8, 9, 10, 11 |
| 2       | 12, 13, 14, 15, 16, 17            | 12, 13                            |
| 3       | 18, 19, 20, 21                    | 14, 15, 16, 17                    |
| 4       | 22, 23, 24                        | 18, 19, 20, 21                    |
| 5       | 25, 26, 27, 28, 29                | 22, 23, 24                        |
| 6       | 30, 31, 32, 33                    | 25, 26                            |
| 7       |                                   | 27, 28, 29                        |
| 8       |                                   | 30, 31, 32, 33                    |

## 5 CASE STUDY

### 5.1 Case Study System

In order to verify the effectiveness of the proposed method, an actual three phase balanced 10 kV radial active distribution network in Zhejiang Province, China, was employed. The feeder has 34 nodes in total. Among them, bus 0 is employed as the reference node, its voltage value is set to 1.05 p.u. The total load in the feeder is 7.3MVA, and a total of 4 MW PVs and 1.2 MW energy storage are added to the network. The topology of the feeder is shown in **Figure 2**.

In this network, the capacity of installed PVs and energy storages are shown in **Tables 1, 2**, respectively.

First, the feeder is modeled by OpenDSS simulation platform, and then the cluster partition and the zonal voltage control are carried out under MATLAB. In order to verify the effectiveness of the proposed method, the day with the largest PV output in 2021 is taken as a typical scenario to be analyzed. The daily maximum PV output is shown in **Figure 3**.

### 5.2 Cluster Partition of the Feeder

Different partition results can be obtained under the comprehensive performance index with different weights. In the cluster partition, different weights can be set for each index according to the experimental conditions. In this study, three weight combinations (numbered C1, C2, and C3) are employed to illustrate the influence of a comprehensive performance index on cluster partition. **Table 3** shows the cluster partition results obtained by different weight combinations.

It can be seen from **Table 3** that as a certain weight creasing, the influence of the corresponding index will be enhanced in the cluster partition. For example, from the weight combination C1 to C2, the weight  $\omega_1$  becomes smaller; meanwhile, the global density function index becomes smaller. It can be known that the value of  $\omega_j$  in **Eq. 10** will be smaller, which means the influence of the global density function index is reduced. Therefore, the weights  $\omega_1$ ,  $\omega_2$ , and  $\omega_3$  should be set according to the experimental

**TABLE 3** | Results of cluster partition under different weight combinations.

| Number | $\omega_1$ | $\omega_2$ | $\omega_3$ | $Q_{GD}$ | $X$    | $M$    | $\omega$ | Number of clusters |
|--------|------------|------------|------------|----------|--------|--------|----------|--------------------|
| C1     | 0.4        | 0.3        | 0.3        | 0.8639   | 0.6637 | 0.7233 | 0.7617   | 6                  |
| C2     | 0.3        | 0.4        | 0.3        | 0.8322   | 0.6866 | 0.7016 | 0.7308   | 7                  |
| C3     | 0.3        | 0.3        | 0.4        | 0.8148   | 0.6748 | 0.7039 | 0.7311   | 7                  |

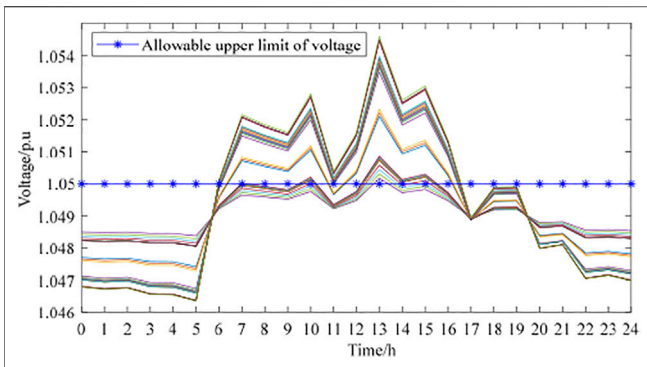


FIGURE 5 | Voltage profile of 10 kV feeder during a day.

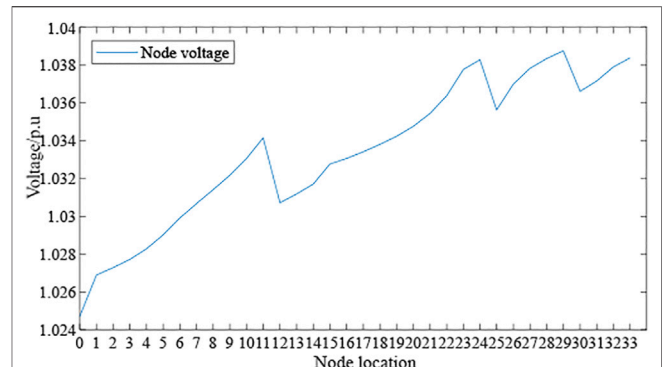


FIGURE 7 | Optimized nodal voltage under the proposed method.

TABLE 5 | Actual outputs of PVs under the proposed method.

| PV           | 11    | 12    | 23    | 24    | 30    | 32      |
|--------------|-------|-------|-------|-------|-------|---------|
| Outputs (kW) | 343.6 | 343.6 | 343.6 | 343.6 | 343.6 | 1,030.9 |

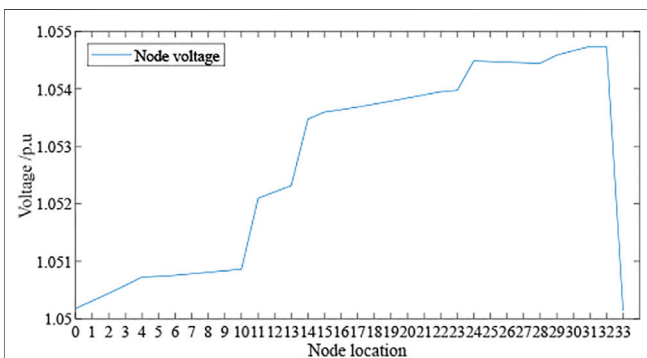


FIGURE 6 | Voltage profile of 10 kV feeder at 13:00.

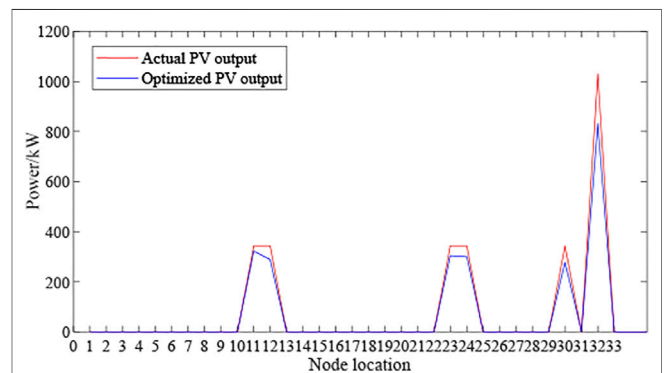


FIGURE 8 | PV outputs under different scenarios.

conditions. According to the actual needs in this study, the cluster partition is analyzed by setting  $\omega_1 = 0.4$ ,  $\omega_2 = 0.3$ , and  $\omega_3 = 0.3$ . The cluster partition results are shown in Figure 4.

It can be seen from Figure 4 that the feeder is partitioned into 6 clusters using the proposed cluster partition method, and there are no isolated nodes exist. Meanwhile, each cluster has the PVs or energy storage, which means each cluster has an adjustable capacity for zonal voltage. To further verify the effectiveness of the proposed method, the modular degree, function  $\rho$  (Li and Yang, 2019) is employed to compare with the comprehensive performance index. Table 4 shows the cluster partition results under the two different indexes.

From Table 4, it can be seen that the feeder can be partitioned into several clusters under the two indexes, and there are no isolated nodes exist. But it should be noticed that under the function  $\rho$ , two clusters have no PVs or energy storage, and the nodal size of the cluster is more unbalanced

than the clusters obtained by comprehensive performance index, which means the proposed a comprehensive performance index can generate a more reasonable cluster partition for subsequent zonal voltage.

### 5.3 Cluster Partition-Based Zonal Voltage Control

Without any voltage regulation measures, the nodal voltage of the feeder is shown in Figure 5. It can be seen from Figure 5 that the voltage of some nodes exceeds the limit at 13:00 noon. To illustrate that the proposed method can effectively adjust the node voltage to a safe operating range, the operating condition of the feeder at 13:00 noon is selected as a typical scenario to be analyzed. In typical scenarios, the actual output of each PVs is shown in Table 5.

In the typical scenario, the solar irradiance comes to the largest during a day, and some nodal voltages exceed the allowable upper limit, which is shown in Figure 6. Under the proposed method, the cluster containing overvoltage nodes is recorded as  $C^V = \{C_1^V, C_2^V, C_3^V, C_4^V, C_5^V, C_6^V\}$ . Under the proposed voltage control method, the profile of nodal voltage and PV outputs are shown in Figures 7, 8, respectively.

It is shown in **Figure 7** that under the proposed voltage strategy, there is no overvoltage existing in the whole network. Meanwhile, **Figure 8** shows that the minimum curtailed PV output is 21.34 kW and the maximum is 198.94 kW, which achieves the goal of maximum PV consumption and avoids the waste of resources.

## 6 CONCLUSION

Aiming at the overvoltage problem caused by the high penetrated PVs, a cluster partition-based zonal voltage control method for the DN is proposed in this study. Considering the structure of DNs, output characteristics of distributed PV in clusters, and the cluster scale, a comprehensive performance index-based cluster partition method is proposed in this study. Based on the community discovery algorithm, the FN algorithm is employed to carry out the partition. The electrical information of the network structure and the impact of PVs on the partitioning solutions are considered, and the size of each subnetwork can be restricted. Based on the cluster partition, an SOCP-based voltage control model aiming at the maximum PV consumption in the cluster is established, and an iterative optimization-based active power coordination strategy among clusters is proposed. The maximum PV consumption for all clusters can be guaranteed, and the

overvoltage problem caused by high penetrated PVs can be effectively solved.

## DATA AVAILABILITY STATEMENT

The original contributions presented in the study are included in the article/Supplementary Material, further inquiries can be directed to the corresponding author.

## AUTHOR CONTRIBUTIONS

XZ: responsible for resources, software, formal analysis, program compilation, and writing—original draft. CX: responsible for writing—review and editing. KP: responsible for methodology, project administration, and funding acquisition. JC: responsible for obtaining the experimental data. XZ: responsible for investigation and resources.

## FUNDING

This study was sponsored by the National Science Foundation for Young Scientists of China (51807026) and Science and Technology Project of Guangzhou Power Supply Bureau of Guangdong Power Grid Corporation (GZHKJXM20190061).

## REFERENCES

- Bi, R., Liu, X. F., Ding, M., Fang, H., Zhang, J. J., and Chen, F. (2019). Renewable Energy Generation Cluster Partition Method Aiming at Improving Accommodation Capacity. *Proc. CSEE* 39 (22), 6583–6592. CNKI:SUN: ZGDC.0.2019-22-010.
- Chai, Y., Guo, L., Wang, C., Zhao, Z., Du, X., and Pan, J. (2007). Network Partition and Voltage Coordination Control for Distribution Networks with High Penetration of Distributed PV Units. *IEEE Trans. Power Syst.* 33, 3396–3407. doi:10.1109/TPWRS.2018.2813400
- Chai, Y. Y., Liu, Y. X., Wang, C. S., Guo, L., Zhao, Z. Z., and Gao, S. (2019). Coordinated Voltage Control for Dis-Tributed PVs Clusters with Incomplete Measurements. *Proc. CSEE* 39 (08), 2202–2212+3. doi:10.13334/j.0258-8013.pcsee.182485
- Cohen, J. (2009). Graph Twiddling in a MapReduce World. *Comput. Sci. Eng.* 11 (4), 29–41. doi:10.1109/mcse.2009.120
- Ding, M., Wang, W. L., Wang, X. L., Song, Y. T., Chen, D. Z., and Sun, M. (2014). A Review on the Effect of Large-Scale Pv Generation on Power Systems. *Proc. CSEE* 34 (01), 1–14. doi:10.13334/j.0258-8013.pcsee.2014.01.001
- Dou, X. B., Chang, L. M., Ni, C. H., Duan, X. M., Ge, P. D., and Wu, Z. J. (2018). Multi-level Dispatching and Control of Active Distribution Network for Virtual Cluster of Distributed Photovoltaic. *Automation Electric Power Syst.* 42 (03), 21–31. doi:10.7500/AEPS20170221007
- Han, Y., Zhang, K., Li, H., Coelho, E. A. A., and Guerrero, J. M. (2018). MAS-based Distributed Coordinated Control and Optimization in Microgrid and Microgrid Clusters: a Comprehensive Overview. *IEEE Trans. Power Electron.* 33 (3), 6488–6508. doi:10.1109/TPEL.2017.2761438
- Hu, X. K., Yin, R., and Shi, M. (2021). Distributed Photovoltaic Cluster Partition and Reactive Power Optimization Strategy Based on Improved Particle Swarm Optimization Algorithm. *Power Capacitor & Reactive*
- Power Compensation* 42 (04), 14–21. doi:10.14044/j.1674-1757.pcrpc.2021.04.003
- Kou, L. F., Xu, Y. H., Hou, X. G., and Zhang, F. (2019). Cluster Partition Method for Large Scale Distributed Photovoltaic in Distribution Network. *Renew. Energ. Resour.* 37 (04), 525–530. doi:10.3969/j.issn.1671-5292.2019.04.009
- Li, S., Wei, Z. N., Sun, G. Q., and Wang, Z. Q. (2018). Stability Research of Transient Voltage for Multi-Machine Power Systems Integrated Lager-Scale PV Power Plant. *Acta Energiae Solaris Sinica* 39 (12), 3356–3362. CNKI:SUN: TYLX.0.2018-12-010.
- Li, X. J., and Yang, J. H. (2019). Research on Realization and Comparison of Community Division Algorithms in Network. *Comput. Digital Eng.* 47 (11), 2861–2865. doi:10.3969/j.issn.1672-9722.2019.11.043
- Liao, Q. P., Lyu, L., Liu, Y. B., Zhang, Y., and Xiong, J. (2017). Reconfiguration Based Model and Algorithm of Voltage Regulating for Distribution Network with Renewable Energy. *Automation Electric Power Syst.* 41 (18), 32–39. doi:10.7500/AEPS20170101003
- Liu, X. F. (2019). *Study on Cluster Partition Method of High Permeability Distributed Renewable Energy Power Generation*. Master's thesis (Hefei, China: Hefei University of Technology).
- Peng, Y., Xiong, W., Yuan, X. F., Zhou, X. S., Shuai, S. X., and Zhao, Z. (2021). Research on Optimal Power Flow of Active Distribution Network Based on Mixed Integer Second-Order Cone Programming. *Electr. Meas. Instrumentation* 2021, 1–7. Available at: <https://kns.cnki.net/kcms/detail/23.1202.TH.20201124.1033.015.html> (Accessed 12 17, 2021).
- Wang, L., Zhang, F., Kou, L. F., Xu, Y. H., and Hou, X. G. (2021). Large-scale Distributed PV Cluster Division Based on Fast Unfolding Clustering Algorithm. *Acta Energiae Solaris Sinica* 42 (10), 29–34. doi:10.19912/j.0254-0096.tynxb.2018-0896
- Xiao, C. L. (2020). *Cluster Partition Based Voltage Control and Optimal Scheduling for Active Distribution Networks*. Doctor's thesis (Hefei, China: Hefei University of Technology).



- Xiao, C. L., Zhao, B., Zhou, J. H., Li, P., and Ding, M. (2017). Network Partition Based Cluster Voltage Control of High-Penetration Distribution Photovoltaic Systems in Distribution Net-Works. *Automation Electric Power Syst.* 41 (21), 147–155. doi:10.7500/AEPS20170101002
- Yan, H. D., Cai, L. H., Sha, J., Lyu, Z. P., and Xu, Z. (2021). Distribution Network Cluster Division and Voltage Control with High Proportion of New Energy Access. *Power Demand Side Manage.* 23 (04), 8–13. doi:10.3969/j.issn.1009-1831.2021.04.003

**Conflict of Interest:** The authors declare that the research was conducted in the absence of any commercial or financial relationships that could be construed as a potential conflict of interest.

**Publisher's Note:** All claims expressed in this article are solely those of the authors and do not necessarily represent those of their affiliated organizations, or those of the publisher, the editors, and the reviewers. Any product that may be evaluated in this article, or claim that may be made by its manufacturer, is not guaranteed or endorsed by the publisher.

*Copyright © 2022 Zhao, Xiao, Peng, Chen and Zhang. This is an open-access article distributed under the terms of the Creative Commons Attribution License (CC BY). The use, distribution or reproduction in other forums is permitted, provided the original author(s) and the copyright owner(s) are credited and that the original publication in this journal is cited, in accordance with accepted academic practice. No use, distribution or reproduction is permitted which does not comply with these terms.*